

## Rediscovering the MJO Extratropical Response: Streamfunction as a Preferred Variable for Subseasonal Teleconnection Analysis

Stephen Baxter<sup>1</sup> and Sumant Nigam<sup>2</sup>

<sup>1</sup>Climate Prediction Center, NOAA/NWS/NCEP, College Park, Maryland

<sup>2</sup>University of Maryland, College Park, MD

### 1. Introduction

Teleconnection analysis serves as a basis for understanding low-frequency (*i.e.* super-synoptic to seasonal) atmospheric variability, and teleconnection patterns serve as building blocks with which one can reconstruct observed atmospheric climate anomalies. While teleconnection analysis has traditionally been conducted to explore recurrent patterns of variability confined to the extratropics (*e.g.* Wallace and Gutzler, 1981; Barnston and Livezy, 1987), there are two clear examples of teleconnection patterns rooted in the subtropics, namely, the atmospheric responses (ranging from the subtropics to the extratropics) to the Madden-Julian Oscillation (MJO) and the El Niño-Southern Oscillation (ENSO). The former is more dominant on subseasonal time scales, while the latter is perhaps the most well-known mode of interannual variability.

The MJO extratropical response can be identified using composite analysis utilizing two different metrics of MJO activity: the popular Wheeler and Hendon (2004) index and a simple velocity potential index derived and monitored by the Climate Prediction Center (CPC). Baxter *et al.* (2014), for example, shows that the MJO can be a useful predictor of subseasonal hydroclimate variability over the contiguous United States, a powerful result given the growing interest in climate prediction that spans the gap between Week-2 forecasts and monthly/seasonal forecasts. That analysis reveals a pattern consistent with various studies highlighting a relationship between the MJO and the Pacific-North America (PNA) pattern as well as the North Atlantic Oscillation (NAO). However, the correlation between the PNA and the MJO (as assessed by either the RMM or CPC index) is modest, on the order of 0.3 or less, as is the correlation between the NAO and MJO. Linear removal of the MJO from the data prior to analysis has little effect on the PNA and NAO patterns. Additionally, a visual inspection of the MJO response pattern and the loading patterns of either the PNA or NAO reveals that there are important differences, and thus the PNA and NAO cannot simply be thought of as an MJO response.

This dilemma is similar to that faced when comparing the PNA and the extratropical response to ENSO. While traditional teleconnection analysis often links PNA and ENSO, an alternative, more physically appropriate analysis reveals that they are quite different. Using 200-hPa geopotential height in a rotated empirical orthogonal function (EOF) analysis yields a PNA pattern as separate from the canonical ENSO response (Nigam, 2003; Nigam and Baxter, 2014). This separation does not readily occur when using 500-hPa geopotential height, as that variable exhibits less tropical and subtropical variance. In that framework then, extratropical variability that is associated with the ENSO response is aliased into the other extratropical patterns of variability, including the PNA. Applying a similar approach to subseasonal teleconnection analysis, however, does not yield an MJO response distinct from teleconnection patterns internal to the extratropical atmosphere. This is likely because the 200-hPa geopotential height variability on subseasonal time scales is much larger at higher latitudes, which are therefore emphasized in an EOF analysis which utilizes the covariance matrix.

The remedy pursued here is to utilize 200-hPa streamfunction, which places the subtropics and the middle and high latitudes on a more equal footing. This is preferred to using the correlation matrix in the EOF analysis since it allows for longitudes that exhibit more variability to be emphasized. The goal of this analysis is to find the MJO extratropical response in the rich spectrum of tropical-extratropical variability.

Additionally, this analysis is targeted toward looking at any tropical footprints of the other known teleconnection patterns. This will involve inspection of various fields in addition to streamfunction, such as velocity potential, outgoing longwave radiation (OLR), and sea-surface temperature (SST). This analysis, we think, will be an important advance in the diagnosis and monitoring of subseasonal teleconnection evolution.

## 2. Data and methods

For this analysis, 200-hPa streamfunction is utilized for the reasons just discussed. A time-extended EOF analysis is utilized to capture the spatio-temporal variability of the 200-hPa streamfunction field at pentad resolution. The analysis period is 35 winter seasons from 1979-2014, and the spatial domain consists of the entire Northern Hemisphere. This analysis focuses on December, January, and February (DJF), the three months that together make up meteorological winter. Winter is therefore taken to be the 19 pentads that span those three months. The data are extended using a five pentad window, and two pentads on each side of the 19-pentad season are allowed into the analysis so that the principal components (PCs) are defined for each of the 19 pentads. The leading eight modes are subject to varimax rotation to allow for more spatial discrimination. The number of rotated modes was selected using a screen test and by using the North *et al.* (1982) criteria. In this framework, a substantial break in the eigenvalues between modes eight and nine occur, beyond which all patterns are likely within the sampling error range. However, to be sure, variants of the

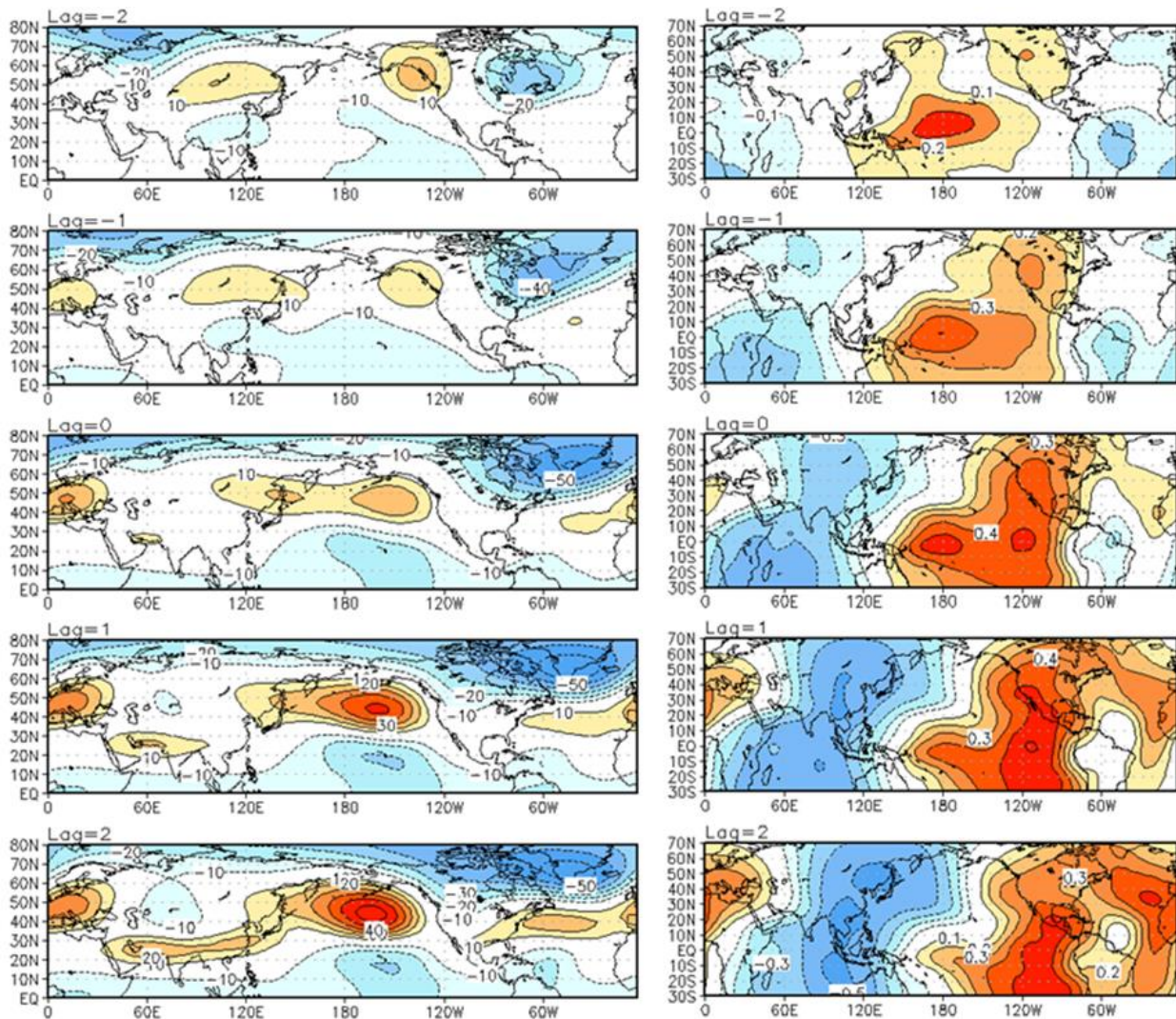


**Fig. 1** Regressions of the 2<sup>nd</sup> PC (9.8% of explained variance) onto 200-hPa geopotential height (left) and correlations with 200-hPa velocity potential (right). This pattern constitutes development of the MJO extratropical response, leading the 1<sup>st</sup> PC by three pentads ( $r=0.9$ ).



analysis are performed rotating as many as ten and as few as six modes. The main results of this analysis are independent of the number of rotated modes, and so the optimal eight modes are retained for this analysis.

The 200-hPa streamfunction, 200-hPa velocity potential, and OLR fields, are all from the latest Climate Forecast System Reanalysis (CFSR, Saha *et al.* 2010). SST data is obtained from a weekly Optimal Interpolation V2 (Reynolds *et al.* 2002) dataset that has been interpolated to pentad resolution. The seasonal cycle is removed from all data where appropriate.

### 3. Results

The results of the rotated, extended EOF analysis of streamfunction reveal the spatio-temporal evolution of several key patterns of subseasonal climate variability. The patterns that are readily identified are the MJO extratropical response, the ENSO response, the North Pacific Oscillation/West Pacific pattern (NPO/WP), the NAO, and the PNA.

The leading two principal components together comprise the MJO response, and together explain 19.9% of the total variance. Figure 1 shows the time evolution from -2 to +2 pentads of the 200-hPa geopotential

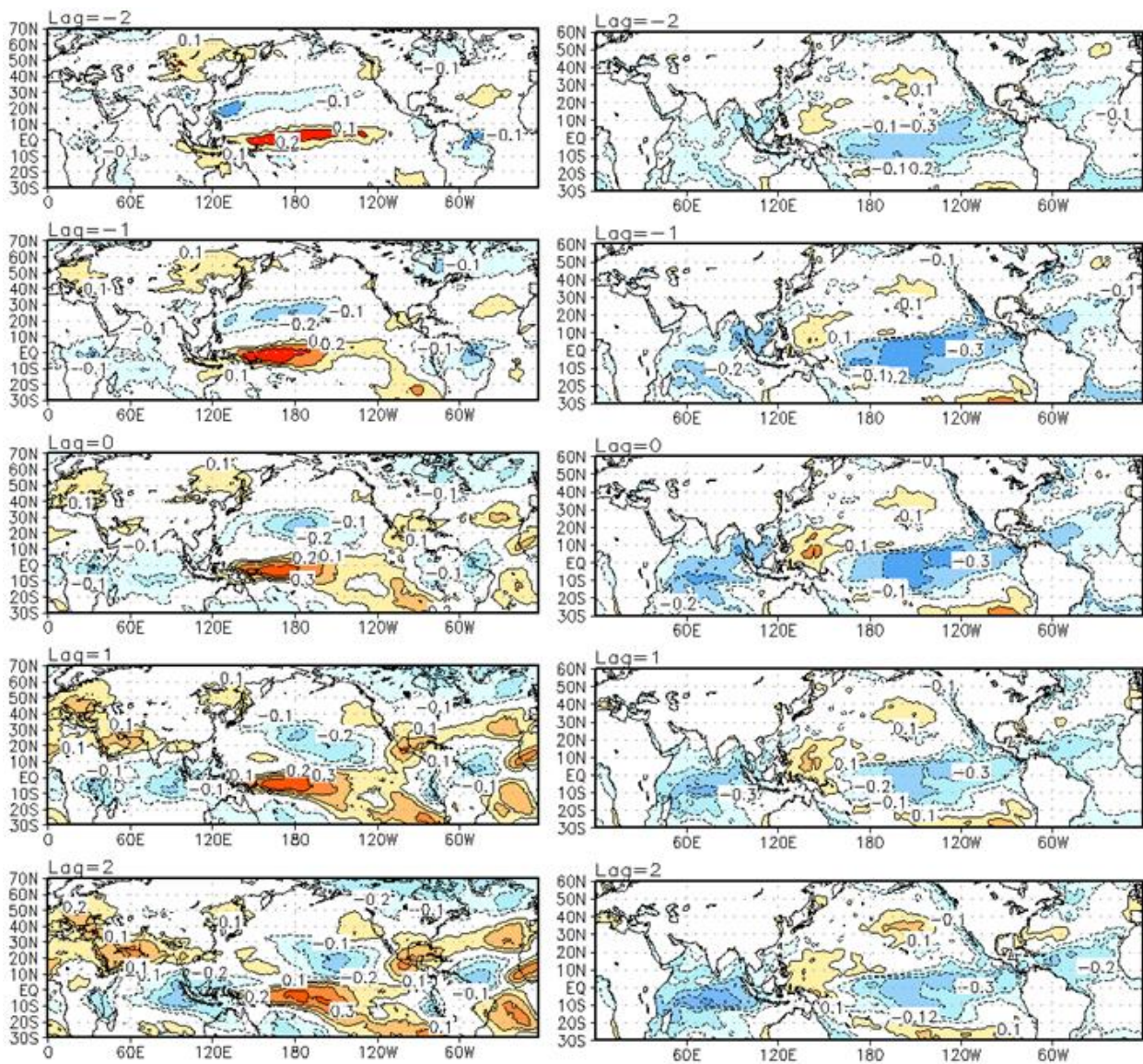


**Fig. 2** Correlations of the 2<sup>nd</sup> PC (9.8% of explained variance), which constitutes the development of the MJO extratropical response, with OLR (left) and SST (right).



height regressions alongside the velocity potential footprints of PC2. PC2 is best characterized as the development of the response pattern, while PC1 (not shown) targets the decay. Not surprisingly, these patterns are highly correlated ( $r=0.9$ ) at a lag of three pentads, with PC2 leading PC1.

These patterns are notable for their robust velocity potential footprints in the tropics, and the development of the MJO extratropical response is associated with, and preceded, by anomalous upper-level convergence (divergence) over the Pacific (Indian Ocean). The development of positive (negative) 200-hPa height anomalies over South Asia (central, subtropical Pacific) is consistent with the anomalous upper-level divergence (convergence) to the south. This is consistent with tropical forcing via the advection of absolute vorticity by the anomalous meridional divergent wind (not shown). Figure 2 shows the OLR and SST footprints associated with the 2<sup>nd</sup> PC, and reveals a dipole of anomalous convection between the Indian Ocean and the west-central Pacific, consistent with this being associated with the MJO. There is some small, but likely significant, relationship with equatorial Pacific SSTs, suggesting some low frequency variability is at play.

It is not surprising that there exists a strong relationship between the leading PCs of this streamfunction analysis and those that intentionally target MJO activity. The correlation between either of the leading PCs and the CPC MJO index (Baxter *et al.* 2014) peaks at  $r=0.62$ , with PC2 leading CPC MJO index 1 (refer to Chapter 2) by one pentad. The final evidence in favor of solidifying the argument that PCs 1 and 2 comprise the MJO extratropical response is a direct, quantitative comparison between the regression pattern obtained in

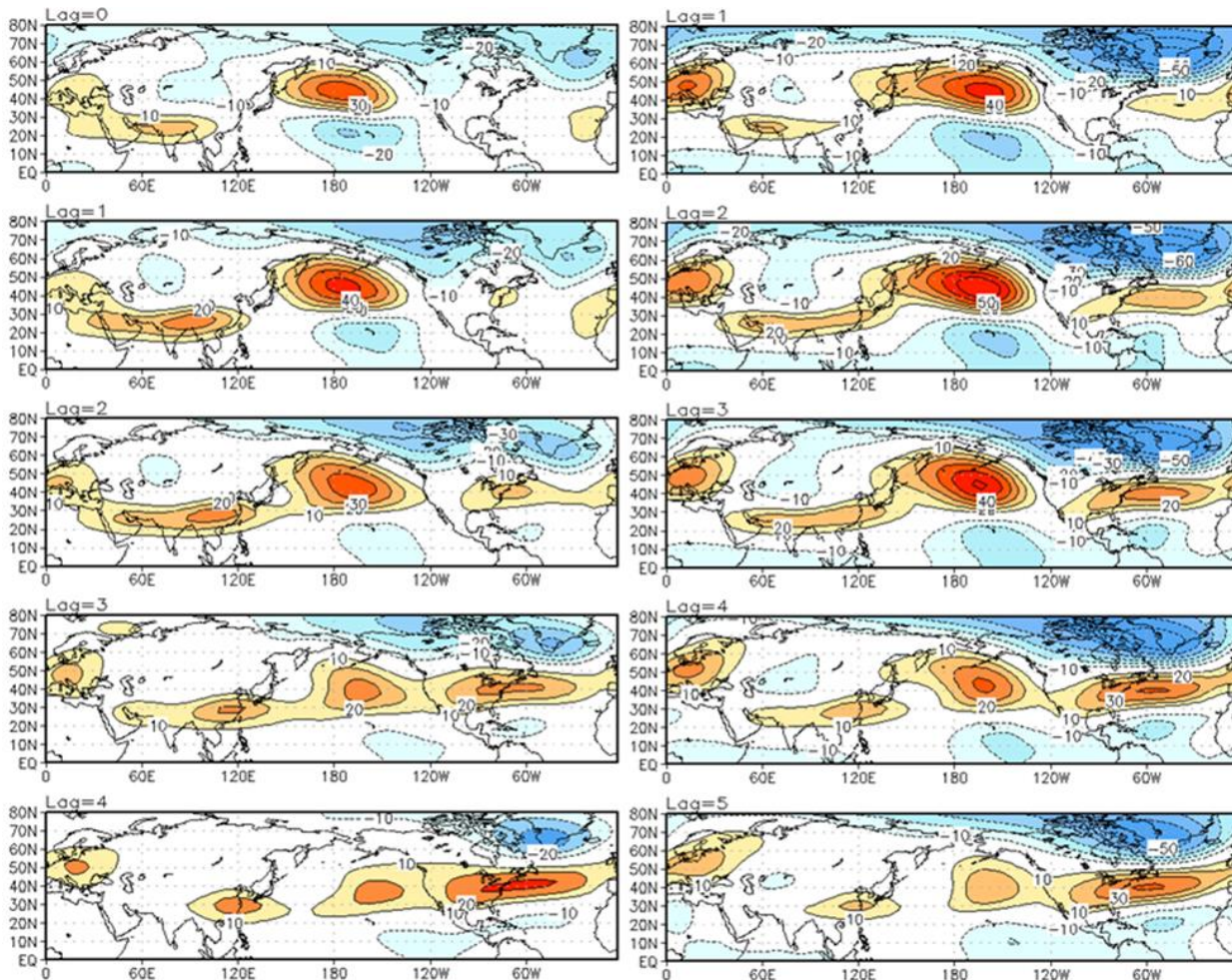


**Fig. 3** Left: Lag regression (lag=0 to lag=4) between CPC MJO Index 1 and the 200-hPa geopotential height. Contour interval is 10m, with the zero contours suppressed. Right: Same as left, but for the 2<sup>nd</sup> PC from the current analysis (lag=1 to lag=5). Spatial correlations are 0.82, 0.82, 0.84, 0.88, and 0.92.



Figure 1 and the regression of CPC MJO index 1 onto the same 200-hPa geopotential height field. Figure 3 shows the regression of CPC MJO index 1 onto the 200-hPa height field from lag=0 to lag=4 pentads. This is plotted alongside the regression of PC2 onto the same height field at lag=1 to lag=5 pentads. The offset is made to put the two indices on par given the one-pentad lag between them. This analysis reveals a striking similarity between the patterns, with spatial correlations from top to bottom of 0.82, 0.82, 0.84, 0.88, and 0.92, respectively. Additionally, the amplitudes of the regressions based on PC2 are higher than in the case of the CPC MJO index (this comparison can be made since both indices are normalized). This is a welcome result, and shows that the MJO extratropical response can be effectively deduced from the data without even direct knowledge of the divergent circulation.

In addition to the MJO circulation response, this analysis also captures the low-frequency ENSO response, manifest on subseasonal timescales. Figure 4 shows the 200-hPa geopotential height and SST patterns associated with the 3<sup>rd</sup> PC. This PC also exhibits the lowest frequency temporal variability, by far, of the eight PCs retained in this analysis. Beyond subseasonal tropical-extratropical teleconnections related the MJO and ENSO, the analysis reveals spatiotemporal variability related to teleconnection more internal to the extratropical atmosphere, including the NAO, the NPO/WP, and the PNA. Further analysis (not shown here) shows that these patterns are not likely generated by anomalous tropical divergent circulations.

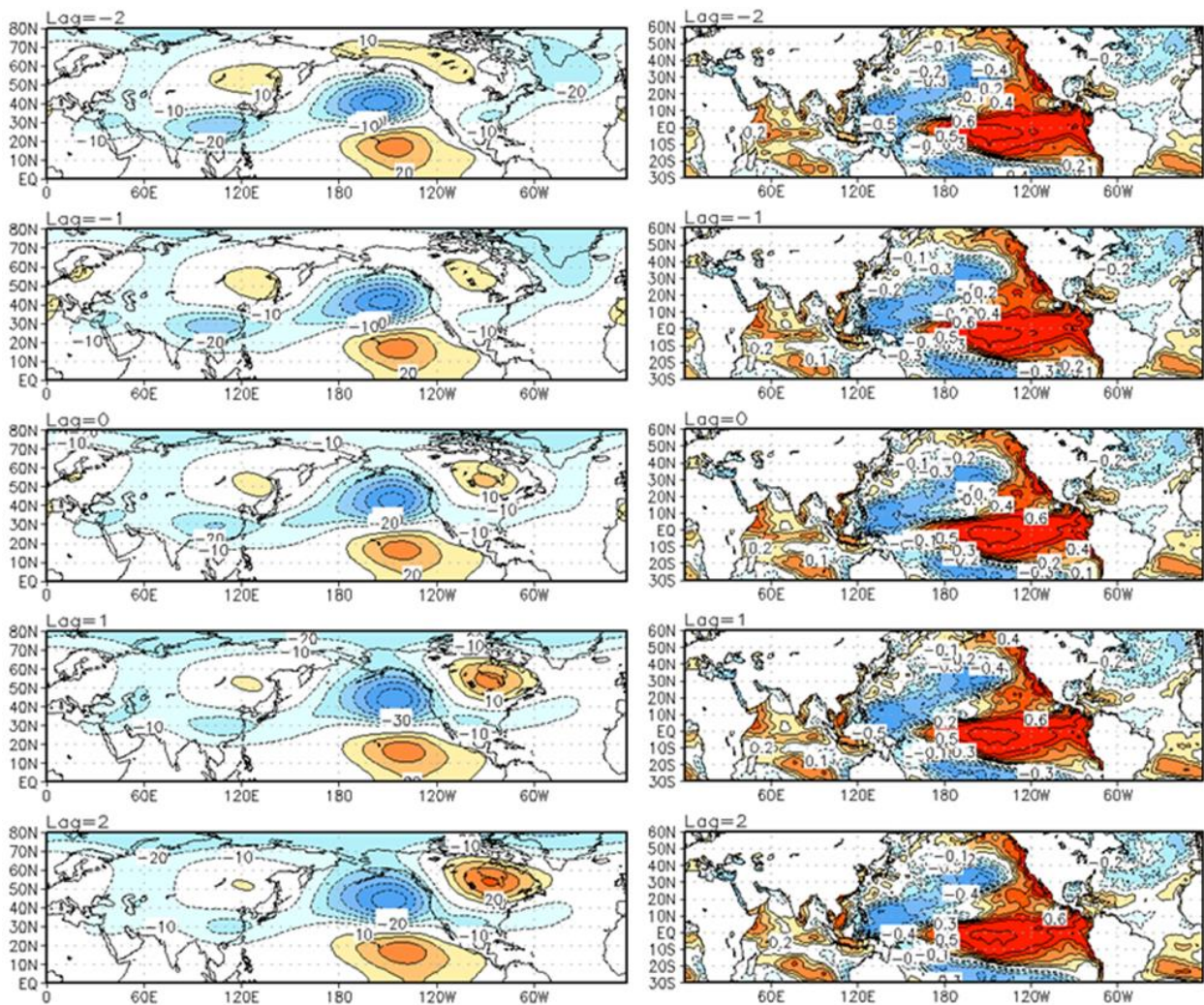


**Fig. 4** Regressions of the 3<sup>rd</sup> PC onto 200-hPa geopotential height (left) and correlations with SST (right). This pattern is clearly recognizable as the extratropical ENSO response.

#### 4. Conclusions

Teleconnection analysis is useful for reconstructing climate anomalies, including quantifying the roles of various patterns in generating climate extremes. Tropical-extratropical teleconnections are of particular interest because of the predictability implied by understanding the mechanisms of subseasonal climate pattern evolution, as they relate to readily observable precursor fields. To this end, analysis of upper-tropospheric streamfunction allows for the identification of the MJO teleconnection within the wide spectrum of tropical-extratropical variability. Subseasonal streamfunction analysis, therefore, is a preferred method for real-time diagnostics and attribution of subseasonal climate variability.

#### References

- Barnston, A., and R. Livezy, 1987: Classification, seasonality, and persistence of low-frequency atmospheric circulation patterns. *Mon. Wea. Rev.*, **115**, 1083–1126.
- Baxter, S., S. Weaver, J. Gottschalck, and Y. Xue, 2014: Pentad Evolution of Wintertime Impacts of the Madden–Julian Oscillation over the Contiguous United States. *J. Climate*, **27**, 7356–7367.
- Nigam, S., 2003: *Teleconnections. Encyclopedia of Atmospheric Sciences*, J. R. Holton, J. A. Pyle, and J. A. Curry, Eds., Academic Press, 2243–2269.
- Nigam, S., and S. Baxter, 2014: *Teleconnections. Encyclopedia of Atmospheric Sciences*, 2nd ed. G. North, Ed., Elsevier Science, 90–109.
- North, G.R., Thomas L. Bell, Robert F. Cahalan, and Fanthune J. Moeng, 1982: Sampling Errors in the Estimation of Empirical Orthogonal Functions. *Mon. Wea. Rev.*, **110**, 699–706.
- Reynolds, R.W., Nick A. Rayner, Thomas M. Smith, Diane C. Stokes, and Wanqiu Wang, 2002: An Improved In Situ and Satellite SST Analysis for Climate. *J. Climate*, **15**, 1609–1625.
- Saha, S., and Coauthors, 2010: The NCEP Climate Forecast System Reanalysis. *Bull. Amer. Meteor. Soc.*, **91**, 1015–1057.
- Wallace, J., and D. Gutzler, 1981: Teleconnections in the geopotential height field during the Northern Hemisphere winter. *Mon. Wea. Rev.*, **109**, 784–804.
- Wheeler, M. C., and H. H. Hendon, 2004: An all-season real-time multivariate MJO index: Development of an index for monitoring and prediction. *Mon. Wea. Rev.*, **132**, 1917–1932.